Spatial trends of nitrate pollution and groundwater chemistry in Shimabara, Nagasaki, Japan

Kei Nakagawa・Hiroki Amano・Hiroshi Asakura・Ronny Berndtsson

K. Nakagawa (✉)・H. Amano・H. Asakura

Graduate School of Fisheries Science and Environmental Studies, Nagasaki University, 1-14 Bunkyo-machi, Nagasaki 852-8521, Japan

e-mail: kei-naka@nagasaki-u.ac.jp

Tel.: +81 95 819 2763; fax: +81 95 819 2763

R. Berndtsson

Division of Water Resources Engineering, Faculty of Engineering, Lund University, Box 118 SE-221 00 Lund, Sweden

Abstract

Groundwater nitrate contamination in agricultural areas is a common problem in many parts of the world. The important agricultural district Shimabara in Nagasaki, Japan, is also experiencing this problem. The general source of drinking water here is groundwater and consequently the nitrate contamination is a big problem. For this reason, a groundwater

investigation was performed and water samples were collected at 40 locations including residential areas, public water supply wells, springs, and rivers from August 2011 to November 2013. Results showed that nitrate nitrogen (NO_3-N) concentration exceeds the Japanese drinking water quality standards (10 mg L^{-1}) at 15 locations. Maximum NO_3-N concentration was 26.6 mg L^{-1}. Nitrate (NO_3^-) is strongly correlated with Cl^- (r =0.96), K^+ (r=0.68), SO_4^{2-} (r=0.66), and Ca^{2+} (r=0.59), respectively. The high correlations with Cl^- and K^+ are related to livestock waste. Corresponding correlation with SO_4^{2-} is related to chemical fertilizers and Ca^{2+} to calcareous material to neutralize acidic soil. Both the first and second components in principal component analysis reflect ion dissolution from aquifer matrix during groundwater flow along the mountain side towards the lower reaches of the alluvial fan. Using hierarchical cluster analysis, chemical characteristics of groundwater were classified into four clusters. One cluster was related to nitrate contaminated groundwater and the other clusters reflected the origin of the major ions in the groundwater.

Keywords

Groundwater, Water chemistry, Nitrate pollution, Principal component analysis, Hierarchical cluster analysis

Introduction

Nitrate contamination of groundwater from agriculture is a common problem in many countries (e.g., Robins 2002; Kaown et al. 2009; Hansen et al. 2012; Nemčić-Jurec et al. 2013; Esmaeli et al. 2014; Rina et al. 2014). Nitrate polluted drinking water may cause health problems such as methemoglobinemia for infants and cancer for adults. World Health Organization (WHO 2011) maximum recommended nitrate ion concentration (NO_3^-) in drinking water is 50 mg L^{-1}. Common pollution sources for nitrate are chemical fertilizers, manure, and domestic wastewater. In Japan nitrate pollution in groundwater is often related to intensive agriculture. The northern part of Shimabara City, Nagasaki Prefecture, has during recent years experienced problems with elevated nitrate concentrations in public water supply wells. In 2005 a committee was established to discuss ways to reduce nitrate pollution for the Shimabara Peninsula (Committee on nitrate reduction in Shimabara Peninsula 2006). The committee recommended changes in agricultural fertilization practices and livestock waste control in the affected regions. However, nitrate nitrogen concentration (NO_3-N) of drinking water is still exceeding recommended maximum values in 23% of all public water supply wells in Shimabara City (Committee on nitrate reduction in Shimabara Peninsula 2011). The Japanese maximum recommended nitrate nitrogen concentration in water supply is 10 mg L^{-1}. In order to better understand the sources and transport patterns of groundwater pollutants we studied the spatial distribution of nitrate pollution together with major chemical elements. For this purpose we collected and analyzed water samples at 40 locations with different area use from August 2011 to November 2013. At specific locations, relationships between precipitation,

groundwater levels, and nitrate concentrations were assessed. Principal component analysis (PCA) and hierarchical cluster analysis (HCA) were used to decipher factors controlling water quality and spatial characteristic of water chemistry.

Materials and Methods

Figure 1 shows the study area and sampling locations. Shimabara City is located in the northeast part of Shimabara Peninsula, Nagasaki, Japan. The area of Shimabara City is 82.8 km^2 occupying about 18% of Shimabara Peninsula. Shimabara City lies on the alluvial fan that spreads on the gentle slopes of Mt. Hugendake in the center of Shimabara Peninsula. Four geological formations represent the Paleogene period. These are, in ascending order, Kazusa, Kitaarima, Tatsuishi (pre-Unzen volcanic rocks), and Unzen volcanic rocks. Kazusa and Kitaarima formations are a part of Kuchinotsu formation, which was shaped in Early Pleistocene. Kazusa formation is composed of deposits including mainly silt, sand, mud, and tuff breccia and Kitaarima formation is composed of marine deposits including mainly sand and sandy silt. Tatsuishi covered Kuchinotu formation, is covering large areas and composed by olivine basalt and two-pyroxene andesite. This formation constitutes the foot of the mountain. Unzen volcanic rock is mainly composed by hornblende andesite dacite (Murakami 1975; Sugimoto 2006).

Figure 2 shows the altitude and land use of Shimabara City. Generally, forest is covering high altitude areas while livestock farms are distributed along mid-slopes of the hills.

Urbanized areas are located at lower altitudes. Agricultural areas are concentrated to the northern parts of Shimabara City. Cultivated areas represented 18.8 km^2 and 23% of Shimabara City in 2010 (Ministry of Agriculture, Forestry and Fisheries, Statistics Bureau 2012). Chinese cabbage, radish, and carrots are major cultivated crops. Double-cropping is conducted by cultivating crops such as potatoes, tomatoes, and onion all year around. Livestock represented 4200 cattle, 30000 pigs, and 937700 chicken in 2010 (Ministry of Agriculture, Forestry and Fisheries, Statistics Bureau 2012). The stock of chicken in Shimabara, e.g., represented 70% of the poultry in Nagasaki Prefecture.

The mean annual precipitation during the observation period was 2541 mm. The highest monthly precipitation was 844.5 mm in July and the lowest monthly precipitation was 27.5 mm in January, 2012 (Japan Meteorological Agency 2014). The average annual temperature is about 17^{o}C. The highest monthly temperature was 28.3^{o}C in August and the lowest monthly average temperature was 6.3^{o}C in February, 2012 (Japan Meteorological Agency 2014).

Sampling locations are shown in Fig. 1. The “RW” represents residential wells, “W” public water supply wells, “O” observation well, “S” springs, and “R” rivers, respectively. The samples for RW-8, 9, 13 and O-1, 2 were collected using a bailer sampler. Other samples were collected from the water tap at locations where wells were not accessible. These water samples were collected after flushing to remove old water in the pipe. For all water sampling polyethylene bottles were used and stored in the refrigerator. Bottles were rinsed thoroughly

with sample water before collecting samples. Main cation and anions (Na^+, K^+, Mg^{2+}, Ca^{2+}, Cl^-, NO_3^-, and SO_4^{2-}) were analyzed by ion chromatography of suppressor type (Metrohm 861 Advanced Compact IC). HCO_3^- was determined by acid-base titration. pH, electrical conductivity (EC), and oxidation-reduction potential (ORP) were measured by a handheld electrode (HORIBA D-52). For this instrument, pH and EC were measured by glass electrode method and dipole electrode method, respectively. The ORP was measured by glass composite electrode including Pt and Ag/AgCl electrodes. The inside of the glass electrode for pH and ORP was filled with 3.33 mol L^{-1} KCl. Dissolved oxygen (DO) was measured by luminescence-based sensor HQd portable meter (HACH HQ30d). Principal component analysis (PCA) and hierarchical cluster analysis (HCA) were used in combination to analyze patterns of chemical elements in the groundwater (e.g., Yidana et al. 2008; Yakubo et al. 2009; Li et al. 2013; Omonona et al. 2014).

Results and Discussion

Water chemistry

Table 1 shows mean of major ion concentrations, NO_3-N, DO, ORP, EC, pH, and well type. DO represents dissolved oxygen concentration in the water that ranged from 6.5 to 9.8 mg L^{-1} with a mean of 9.1 mg L^{-1}. Standard deviation of DO ranged from 0.2 to 1.8 mg L^{-1} with a mean of 1.0 mg L^{-1}. The DO for all sampling sites were above 2 mg L^{-1} which is suitable for

aerobic bacteria. The ORP represented redox status ranging from 172.5 to 282.0 mV with a mean of 216.0 mV. Standard deviation of ORP ranged from 12.0 to 91.4 mV with a mean of 61.2 mV. The ORP was positive, indicating that all collected water samples are in oxidation state. The EC depending on ion quantity ranged from 7.7 to 49.7 mS m^{-1} with a mean of 28.8 mS m^{-1}. Standard deviation of EC ranged 1.2 to 14.6 mS m^{-1} with a mean of 6.5 mS m^{-1}. EC had high positive correlation with total ion concentration ($mmol_c$ L^{-1}) (r = 0.95). pH ranged from 6.4 to 7.8 with a mean of 7.0. Standard deviation of pH ranged from 0.0 to 0.6 with an average of 0.3. pH varied from slightly acidic to slightly alkaline.

A trilinear diagram for all 277 water samples is shown in Fig. 3. All samples except RW-b were classified into Ca-HCO_3 (area Ⅰ) or Ca-(SO_4+NO_3) (area Ⅲ). Samples such as W7-9 and S-1, collected from a forest area, were classified into Ca-HCO_3 type. Samples from W-14~20, S-2, 3 and RW-1~3, collected from suburban and urban areas, were also classified into Ca-HCO_3. The Ca-HCO_3 type is the most common for shallow groundwater in Japan. Samples from RW-7~9, 11, 13 and 14, O-1, 2, R-2 and W-1~5 were collected from agricultural areas and here NO_3-N concentration exceeded Japanese recommended drinking water quality standard (10 mg L^{-1}) for most of these locations. These samples were classified into Ca-(SO_4+NO_3). According to the above results, the original groundwater is classified into Ca-HCO_3 while nitrate polluted groundwater is classified into Ca-(SO_4+NO_3).

Figure 4 shows stiff diagrams for the 40 sampling locations. At sampling locations with altitude from 300 to 400 m, the ion concentration was very low and the smaller the area of

the polygonal shape because of the location close to mountainside recharge areas. As altitude decreases, ion concentrations tend to increase. This indicates that ion dissolution from the matrix occurs during groundwater flow. Ca^{2+} was the most common cation for most locations. A few locations had higher contents of Na^{+}+K^{+} or Mg^{2+}. Probably, cation exchange or other kinds of mineral dissolution occur in these locations.

Spatial and temporal trends of NO_3-N concentration

Mean and standard deviation of NO_3-N concentrations are shown in Fig. 5. NO_3-N concentration ranged from 0.1 to 25.8 mg L^{-1} with an average of 8.8 mg L^{-1}. Maximum standard deviation was 3.52 mg L^{-1} at O-2. Large standard deviations were found at RW-8, 9, 13, O-1, 2, and W-3. RW-13 and W-3 are located halfway up on the mountainside. Other locations represent discharge areas close the sea shore. The NO_3-N concentration at 15 locations exceeded Japanese drinking water quality standards (10 mg L^{-1}; maximum at RW-11 with 25.8 mg L^{-1}). However, NO_3-N concentration at 21 locations exceeded the threshold 3 mg L^{-1} considered as contaminated by human activity (Eckhardt and Stackelberg 1995).

The variation in groundwater chemistry is mainly due to groundwater recharge, pumping, and geochemical reactions. Rajmohan et al. (2005) reported that an increasing groundwater level affected by rainfall means a nitrate concentration increase and decrease with receding groundwater level. A comparison between groundwater table elevation, NO_3-N concentration, and daily precipitation for RW-8, RW-9, and RW-13 is shown in Fig. 6. The

figure shows that groundwater table increase resulted in NO_3-N concentration decrease at RW-8 on June 19, 2012. The NO_3-N concentration decreased due to dilution from groundwater recharge and large amounts of precipitation (275.5 mm) from June 15 to 16, 2012. A significant groundwater table increase was observed at RW-8 in August 5, 2013, which was a result of 35.5 mm precipitation the day before. In this case, NO_3-N concentration increased. This was due to the flushing of nitrate by recharging groundwater. The groundwater table elevation in June 19, 2012, was lower than that in August 5, 2013. Probably the peak concentration in the groundwater was not sampled for this event. On June 19, 2012, and August 5, 2013, the groundwater table increased and the NO_3-N concentration decreased simultaneously at RW-9. This was due to dilution by groundwater as well as for the case of RW-8. A rise in the groundwater table at RW-13 was observed in August 22, 2012. This was a result of 100.5 mm precipitation from August 8 to 14, 2012. The NO_3-N concentration decreased by dilution related to the precipitation. According to the above results, recharging precipitation is the most important factor controlling groundwater table changes and NO_3-N concentration in this area.

The spatial distribution of NO_3-N concentration is shown in Fig. 8. High NO_3-N concentrations (above 10 mg L^{-1}) are mainly observed in the northern parts of Shimabara City. When comparing to Fig. 2, high NO_3-N concentrations coincide with the spatial distribution of agricultural areas. Sampling locations in forested, urban, and suburban areas do not show high NO_3-N concentration. This reveals that agricultural activities are related to nitrate pollution in the study area. Using statistical data on agriculture and forestry (Ministry of Agriculture,

Forestry and Fisheries, Statistics Bureau, 2007), we analyzed nitrate load potential for each village in 2005 (Nakagawa et al. unpublished). The area cover of each village is shown in Fig. 1. Nitrate load potential was estimated from the amount of livestock waste and applied chemical fertilizer according to these statistics. High potential of nitrate load from livestock waste was estimated for villages at 300-400 m altitude. The location of these villages are close to S-1 and W-6~10. Estimated maximum nitrate load potential was 305041 kg N/year. The nitrate load potential from livestock waste (1442043 kg N/year) was much higher than that from chemical fertilizers (258520 kg N/year), at the city total. Therefore, livestock waste can be assumed to be a main source of nitrate pollution in the area. This is confirmed by observed high NO_3-N concentration downstream potential high load nitrate villages.

Correlation of major ions

Correlation coefficients between major ions for all 277 samples are shown in Table 2. NO_3^- was positively correlated with Cl^- (correlation coefficient r=0.96), K^+ (r=0.68), SO_4^{2-} (r=0.66), and Ca^{2+} (r=0.59). Livestock waste includes Cl^- and essential nutrients such as N, P, and K. Jalali (2011) reported that high NO_3^- and Cl^- contamination in groundwater indicates effects applied manure and livestock waste. Thus, positive correlation with Cl^- and K^+ may reflect application of manure and leakage of livestock wastes from composting facilities.

The positive correlation between NO_3^- and SO_4^{2-} may reflect application of chemical fertilizers such as $(NH_4)_2SO_4$ (Babiker et al. 2004). Babiker et al (2004) reported that high

positive correlation was found between NO_3^-, Mg^{2+}, and Ca^{2+}, which indicates their origin from chemical fertilizers such as $CaCO_3$ and $MgCO_3$ In this study, the positive correlation between NO_3^- and Ca^{2+} indicates the use $CaCO_3$ in the area.

In Japan, calcareous material is often used for neutralization of pH against soil acidification. The positive correlation between NO_3^- and Ca^{2+} may indicate application of calcareous material in connection to crop production.

The correlation between NO_3^- and Mg^{2+} was 0.32 only. However, the correlation became 0.80 at the NO_3^- concentration above 13 mg L^{-1}. The relationship is related to use of $MgCO_3$ as a chemical fertilizer. The threshold of NO_3^- concentration when considering contamination due to human activity is about 13 mg L^{-1} (Eckhardt and Stackelberg 1995). For conditions of low NO_3^- concentration (below 13 mg L^{-1}), dissolution of minerals which are included in biotite, amphibole, plagioclase, and olivine may contribute to the increasing K^+, Ca^{2+}, and Mg^{2+}. These components are highly correlated with each other.

Negative correlation between NO_3^- and HCO_3^- (r=-0.53) is one of the factors that is indicating the occurrence of denitrification (e.g., Mohamed et al. 2003). Denitrification occurs in the presence of organic carbon and in a reducing environment with little oxygen. The denitrification process can be expressed as:

$$4NO_3^- + 5C + 2H_2O \rightarrow 2N_2 + 4HCO_3^- + CO_2 \quad (1)$$

This means that HCO_3^- increases with decreasing NO_3^-. However, the observations did not indicate this relationship. Moreover, the DO and ORP data (Table 1) suggests that the

groundwater in this area is not under redox condition. Thus, it may be concluded that denitrification is not an important process for the investigated area.

Principal component analysis and hierarchical cluster analysis

The input of 8 variables (major ions Cl^-, NO_3^-, SO_4^{2-}, HCO_3^-, Na^+, K^+ Mg^{2+}, and Ca^{2+}) was used to perform a combined analysis using principal components analysis (PCA) and hierarchical cluster analysis (HCA). The input data was standardized before analysis. The correlation between the variables were used to calculate eigenvalue, factor loading, and principal component scores. HCA was based on Ward's method with squared Euclidean distance (e.g., Yakubo et al. 2009; Omonona et al. 2014). The results of the PCA are shown in Table 3. The total number of components (common factors) in the PCA was determined based on the Kaiser criterion (Cloutier et al. 2008). In this criterion, only the components with eigenvalues greater than 1 are retained. Two principal components were extracted, accounting for most of total variance (87%). Hereafter, the first principal component is called Factor 1 and the second Factor 2, respectively.

Factor 1 has high positive loading for Cl^-, NO_3^-, SO_4^{2-}, Na^+, K^+, Mg^{2+}, and Ca^{2+} (0.73~0.92), and represents 60% of total variance. Figure 8 shows the relationship between the two principal components (Factor 1 and 2) and the ion concentration. Factor 1 represents increasing NO_3^- concentration due to livestock waste, application of manure, and chemical fertilizer (Fig. 8a~c). There are low concentration horizontal distribution of NO_3^- and Cl^-

associated with Factor 1. However, SO_4^{2-}, Na^+, K^+, Mg^{2+}, and Ca^{2+} concentrations rerated to this distribution are plotted to show the increasing general trend. Thus, the increase of ion concentration associated with Factor 1 except for NO_3^- and Cl^- is also related to contribution from the same origin and ion dissolution during groundwater flow (Fig. 8a~c). Factor 2 has negative loading for Cl^- and NO_3^- (-0.50 and -0.60, respectively) and positive loading for HCO_3^-, Na^+, and Mg^{2+} (0.53~0.97), representing 27% of the total variance. Although Factor 2 has negative correlation with NO_3^- and Cl^-, almost no relationship can be seen in Fig. 8d. Increase in concentration for HCO_3^-, Na^+, and Mg^{2+} associated with Factor 2 (Fig. 8e) is due to ion dissolution during groundwater flow. Both Factor 1 and 2 represent ion dissolution from aquifer matrix during groundwater flow from the mountain side to downstream. Additionally, Factor 1 also explains the effect of nitrate pollution.

For the HCA, all 277 water samples were classified into four clusters. Hereafter, these clusters are called Group 1 to 4. Averaged major ion concentration for each group is shown in Table 4. Group 1, 2, and 3 show low NO_3^- concentration below 13 mg L^{-1}. When comparing ion concentrations for Group 1-3, all ions except for Cl^- and NO_3^- concentration were in order Group 2>1>3. The difference for all ion concentrations belonging to each group except for Cl^- and NO_3^- is clear and shows the pristine water chemistry. Group 4 shows high NO_3^- concentration due to nitrate pollution (NO_3-N exceeding 10 mg L^{-1}). Therefore, the groups can be divided into two main water types. Group 1, 2, and 3 thus represent not-contaminated water and Group 4 nitrate polluted water.

When we look at group association over time and depending on spatial location, water samples keep the same cluster over the entire study period except for water samples at W-17. These can be classified either into Group 1 or 3 depending on the sampling time. However, W-17 does not show any seasonal changes. Figure 9 shows the spatial distribution of the groups based on the latest data in the study period. Group 1 and 2 cover the urban and suburban areas. Group 3 covers mainly forested areas at higher altitude. Finally, Group 4 covers agricultural areas.

Figure 10 shows all samples in a trilinear diagram divided into the groups. A seen from the figure Group 1 and 2 can be classified into Ca-HCO_3 (area Ⅰ) and Group 4 into Ca-(SO_4+NO_3) (area Ⅲ). Group 3 is classified into both Ca-HCO_3 (area Ⅰ) and Ca-(SO_4+NO_3) (area Ⅲ). Although water samples such as W-12 and W-13 are classified into Group 3, this water is probably changing chemical characteristics over time so as to transit from pristine to polluted water. The sampling locations W-12 and W-13 were close to polluted samples classified into Group 4 (see Fig. 9)

Figure 11 shows a scatter plot of all water samples against principal components (Factor 1 and 2) and divided into groups. If the factor score is greater than 0, the processes represented by the component have significant influences on the water chemistry at the location. On the other hand, if the factor score is less than 0, the processes represented by the factor probably do not have any significant influence on the water chemistry at that location (e.g., Yakubo et al. 2009). According to the figure, Group 4 is influenced by Factor 1 only. Most

samples of Group 1 are influenced by Factor 2 (dissolution of ions). Some samples of Group 1 and all samples of Group 2 are influenced by common effects (dissolution of ions), Factor 1 (dissolution of ions and nitrate pollution), and Factor 2 (dissolution of ions). These two factors do not have significant influence on the samples of Group 3. Thus, all groups except Group 3 must be controlled by ion dissolution and/or nitrate pollution.

Conclusion

To understand present status of nitrate contamination and determine the factors controlling the water chemistry in Shimabara, water samples were collected and analyzed regarding major ion component in private and public water supply wells, springs, and rivers. The main findings were as follows: (1) According to the average NO_3-N concentration 15 out of 40 locations (38% of all sampling locations) exceeded 10 mg L^{-1} (Japanese drinking water quality standard). The concentration at 21 locations (53% of all sampling locations) exceeded the threshold value of 3 mg L^{-1} and can be considered as contaminated due to human activity. The contaminated sampling positions are all located downstream of potential high nitrate load areas, (2) Water samples were classified into Ca-HCO_3 or Ca-(SO_4+NO_3) type, and water quality changed from Ca-HCO_3 to Ca-(SO_4+NO_3) type due to nitrate pollution, (3) The positive correlation between NO_3^- and ions such as Cl^-, K^+, and SO_4^{2-} indicate that nitrate pollution in groundwater is caused by livestock waste and over-application of manure and chemical fertilizers, (4) At some locations, the water table in water supply wells was clearly influenced

by infiltrating precipitation. Thus, nitrate concentration was diluted by the recharge from infiltration, (5) The PCA indicated that water chemistry is controlled by two main factors. Both factors are related to ion dissolution during groundwater flow. One of these factors is also influenced by nitrate pollution, and (6) According to the HCA, water samples can be classified into four spatial groups. The water chemistry in one of these is controlled by nitrate pollution and ion dissolution, whereas two groups are affected by only ion dissolution. The factors obtained from PCA have no significant influence on the final group.

To conclude, our study shows the characteristics of groundwater chemistry in Shimabara is divided into four clusters. Especially, the nitrate polluted cluster is clearly different from the other clusters. The nitrate polluted areas are confined to the northern parts of Shimabara City. Therefore, the contaminant sources must be located upstream of this area. Countermeasures should be performed to improve the water quality. This can be done by more detailed groundwater flow and contaminant transport analyses. Results from this paper can be used to design such a groundwater flow and contaminant transport analysis.

Acknowledgements

This work was supported by JSPS KAKENHI Grant Number 24360194.

References

Babiker IS, Mohamed MAA, Terao H, Kato K, Ohta K (2004) Assessment of groundwater contamination by nitrate leaching from intensive vegetable cultivation using geographical information system. Environ Intern 29:1009-1017. doi:10.1016/S0160-4120(03)00095-3

Cloutier V, Lefebvre R, Therrien R, Savard MM (2008) Multivariate statistical analysis of geochemical data as indicative of the hydrogeochemical evolution of groundwater in a sedimentary rock aquifer system. J Hydrol 353:294-313. doi:10.1016/j.jhydro.2008.02.015

Committee on nitrate reduction in Shimabara Peninsula (2006) Shimabara peninsula nitrate load reduction project (in Japanese), 131p

Committee on nitrate reduction in Shimabara Peninsula (2011) The second term of Shimabara peninsula nitrate load reduction project (in Japanese). 105p

Eckhardt DAV, Stackelberg PE (1995) Relation of Ground-Water Quality to Land Use on Long Island, New York. Groundwater 33(6):1019-1033. doi:10.1111/j.1745-6584.1995.tb00047.x

Esmaeili A, Moore F, Keshavarzi B (2014) Nitrate contamination in irrigation groundwater, Isfahan, Iran. Environ Earth Sci 72(7):2511-2522. doi:10.1007/s12665-014-3159-z

Hansen B, Dalgaard L, Thorling L, Sørensen B, Erlandsen M (2012) Regional analysis of groundwater nitrate concentrations and trends in Denmark in regard to agricultural influence. Biogeosci 9:3277-3286. doi:10.5194/bg-9-3277-2012

Jalali M (2011) Nitrate pollution of groundwater in Toyserkan, western Iran. Environ Earth Sci 62:907-913. doi:10.1007/s12665-010-0576-5

Japan Meteorological Agency (2014) Weather observation data. Japan Meteorological Agency Web. <http://www.jma.go.jp/jma/index.html> (accessed 14.01.14)

Kaown D, Koh DC, Mayer B, Lee KK (2009) Identification of nitrate and sulfate sources in groundwater using dual stable isotope approaches for an agricultural area with different land use (Chuncheon, mid-eastern Korea). Agriculture, Ecosystem and Environment 132:223-231. doi:10.1016/j.agee.2009.04.004

Li P, Qian H, Wu J, Zhang Y, Zhang H (2013) Major Ion Chemistry of Shallow Groundwater in the Dongsheng Coalfield, Ordos Basin, China. Mine Water Environ 32:195-206. doi:10.1007/s10230-013-0234-8

Ministry of Agriculture, Forestry and Fisheries, Statistics Bureau., 2007. 2005 Census of agriculture and forestry Volume 1 No 42, Nagasaki Prefecture Statistics Report (in Japanese). 130p

Ministry of Agriculture, Forestry and Fisheries, Statistics Bureau., 2012. 2010 World census of agriculture and forestry Vol 1 No 42, Nagasaki Prefecture Statistics Report (in Japanese). 125p

Mohamed MAA, Terao H, Suzuki R, Babiker IS, Ohta K, Kaori K, Kato K (2003) Natural denitrification in the Kakamigahara groundwater basin, Gifu prefecture, central Japan. Sci Tot Environ 307:191-201. doi:10.1016/S0048-9697(02)00536-3

Murakami T (1975) Hydrogeological Map of Shimabara Peninsula 1:50,000 (in Japanese). Geol Surv Japan 25:1

Nemčić-Jurec J, Konjačić M, Jazbec A (2013) Monitoring of nitrates in drinking water from agricultural and residential areas of Podravina and Prigorje (Croatia). Environ Monit Assess 185:9509-9520. doi:10.1007/s10661-013-3269-1

Omonona OV, Onwuka OS, Okogbue CO (2014) Characterization of groundwater quality in three settlement areas of Enugu metropolis, southeastern Nigeria, using multivariate analysis. Environ Monit Assess 186:651-664. doi:10.1007/s10661-013-3405-y

Rajmohan N, Elango L (2005) Nutrient chemistry of groundwater in an intensively irrigated region of southern India. Environ Geol 47:820-830. doi:10.1007/s00254-004-1212-z

Rina K, Datta PS, Singh CK, Mukherjee S (2014) Determining the genetic origin of nitrate contamination in aquifers of Northern Gujarat, India. Environ Earth Sci 71:1711-1719. doi:10.1007/s12665-013-2575-9

Robins NS (2002) Groundwater quality in Scotland: major ion chemistry of the key groundwater bodies. Sci Tot Environ 294:41-56. doi:10.1016/S0048-9697(02)00051-7

Sugimoto T (2006) Geology and Petrology at Shimabara Peninsula, Kyushu, SW Japan -From recent results- (in Japanese). J Geotherm Res Soc Japan 28(4):347-360

WHO (World Health Organization) (2011) Guidelines for drinking water quality, 4th edn

Yakubo BB, Yidana SM, Nti E (2009) Hydrochemical Analysis of Groundwater Using Multivariate Statistical Methods-The Volta Region, Ghana. KSCE J Civ Engin 13(1):55-63. doi:10.1007/s12205-009-0055-2

Yidana SM, Ophori D, Yakubo BB (2008) A multivariate statistical analysis of surface water chemistry data-The Ankobra Basin, Ghana. J Environ Manag 86:80-87. doi:10.1016/j.jenvman.2006.11.023

Figure Captions

Fig. 1 Location of the study area and sampling points

Fig. 2 Land use map of the study area; (a) Altitude, and (b) Land use

Fig. 3 Trilinear diagram for 277 samples in the study area

Fig. 4 Distribution of stiff diagrams for 40 sampling points

Fig. 5 Mean values and standard deviation of NO_3-N for 40 sampling points

Fig. 6 NO_3-N concentration and water table elevation at RW-8, RW-9 and RW-13 and daily precipitation during the study period

Fig. 7 Distribution of NO_3-N concentration

Fig. 8 Relationship between two principal components and ion contents; (a) Factor 1 vs. SO_4^{2-}, Cl^-, and NO_3^-, (b) Factor 1 vs. Na^+ and K^+, (c) Factor 1 vs. Mg^{2+} and Ca^{2+}, (d) Factor 2 vs. Cl^- and NO_3^-, and (e) Factor 2 vs. HCO_3^-, Na^+ and Mg^{2+}

Fig. 9 Distribution of respective clusters

Fig. 10 Trilinear diagram of 277 samples divided into clusters

Fig. 11 Scatter plot for two principal components and respective clusters

Table captions

Table 1 Mean values of anions, cations, NO_3-N, DO, ORP, EC, pH, and well type

Table 2 Correlation between eight ion contents

Table 3 Results of principal component analysis

Table 4 Mean concentrations of respective clusters

Table 1 Mean values of anions, cations, NO_3-N, DO, ORP, EC, pH, and well type

	Number of samples	Cl^- (mg L^{-1})	NO_3^- (mg L^{-1})	SO_4^{2-} (mg L^{-1})	HCO_3^- (mg L^{-1})	Na^+ (mg L^{-1})	K^+ (mg L^{-1})	Mg^{2+} (mg L^{-1})	Ca^{2+} (mg L^{-1})	NO_3-N (mg L^{-1})	DO (mg L^{-1})	ORP (mV)	EC (mS m^{-1})	pH	Well type
RW-1	1	16.4	25.9	15.2	118.5	30.9	4.8	4.4	30.3	5.9	N.M.	N.M.	38.0	6.8	S
RW-2	1	6.0	8.1	8.3	138.4	10.7	7.1	12.4	22.3	1.8	N.M.	N.M.	33.0	6.5	D
RW-3	1	9.3	0.5	16.7	111.9	22.3	4.7	7.6	21.7	0.1	N.M.	N.M.	30.0	7.3	S
RW-7	8	23.9	104.5	37.0	24.6	16.3	10.5	10.8	34.6	23.6	7.9	195.5	48.7	6.9	D
RW-8	11	18.2	67.0	40.0	37.4	12.7	12.8	6.9	35.7	15.1	6.5	242.3	37.3	6.7	S
RW-9	10	16.6	68.9	23.9	29.4	13.2	8.2	9.6	23.9	15.6	8.5	228.9	42.9	6.6	S
RW-11	2	18.9	114.4	9.8	23.2	13.0	13.2	8.7	22.3	25.8	N.M.	N.M.	33.0	6.5	D
RW-12	1	10.8	20.0	5.5	27.8	6.8	2.9	3.8	12.7	4.5	N.M.	N.M.	9.9	6.6	D
RW-13	11	23.2	97.2	57.3	12.1	11.3	8.9	11.4	42.1	22.0	9.3	211.7	49.7	6.5	S
RW-14	2	18.3	62.5	38.1	37.9	21.7	5.5	10.8	23.4	14.1	8.8	172.5	32.1	7.3	D
RW-a	8	24.7	99.1	22.5	26.7	16.7	8.2	11.9	29.0	22.4	8.9	211.1	48.0	7.1	
RW-b	1	10.3	21.4	32.2	64.8	23.3	10.3	4.8	14.0	4.8	9.5	212.0	30.7	7.2	
O-1	6	24.2	81.4	33.6	39.7	16.4	9.1	11.9	36.1	18.4	7.4	188.0	46.1	7.1	-
O-2	6	23.4	79.9	31.3	42.4	17.0	8.5	11.7	35.1	18.1	7.9	174.5	47.0	7.2	-
R-1	1	7.5	26.2	15.6	32.6	5.3	7.2	4.0	19.5	5.9	N.M.	N.M.	21.0	6.7	-
R-2	1	19.1	74.8	36.3	47.0	15.5	9.4	9.8	31.9	16.9	9.7	272.0	45.0	7.8	-
S-1	5	3.3	1.1	1.8	37.6	6.3	3.4	1.7	6.1	0.2	9.3	26.8	12.9	7.0	D
S-2	1	5.4	11.7	6.3	83.0	8.5	4.9	7.6	16.1	2.6	9.0	282.0	23.6	6.4	-
S-3	1	5.7	11.5	6.1	77.2	8.6	4.8	6.8	15.2	2.6	9.0	233.0	20.5	6.4	-
S-4	1	13.0	11.6	9.9	128.3	11.5	6.6	15.4	27.6	2.6	N.M.	N.M.	N.M.	N.M.	-
W-1	10	15.8	55.6	25.4	44.2	12.3	5.8	10.3	22.8	12.6	9.5	221.3	32.2	7.4	D

W-2	10	14.4	36.4	25.8	34.8	11.5	4.8	8.1	18.6	8.2	9.2	208.4	25.9	7.3	D
W-3	10	18.2	61.1	40.3	27.7	14.0	6.4	10.5	25.9	13.8	9.4	217.3	34.9	7.2	D
W-4	9	24.4	77.6	50.6	25.0	16.5	7.4	12.9	30.0	17.5	9.6	208.8	41.2	7.1	D
W-5	10	21.0	77.0	44.0	20.9	15.8	7.6	11.3	28.0	17.4	9.5	207.0	37.5	7.0	D
W-6	10	3.9	6.3	2.2	45.1	6.5	3.4	3.4	8.3	1.4	9.4	216.3	11.0	7.4	D
W-7	9	3.8	2.2	0.9	42.1	6.2	3.7	2.8	7.4	0.5	9.4	227.1	9.1	7.4	
W-8	10	3.7	1.2	0.7	35.3	5.8	3.1	2.3	5.7	0.3	9.6	222.4	7.9	7.3	D
W-9	10	3.6	0.5	0.6	36.9	6.5	2.9	2.3	5.7	0.1	9.6	216.7	7.7	7.3	
W-10	10	5.1	13.5	3.0	32.0	6.3	4.1	3.0	8.0	3.1	9.8	211.9	11.2	7.2	D
W-11	10	18.8	64.5	18.9	35.9	13.4	8.6	8.9	22.3	14.6	9.7	202.9	31.0	7.0	D
W-12	10	6.8	18.8	7.8	38.7	8.1	4.1	4.7	12.2	4.2	9.6	205.5	14.9	7.4	D
W-13	10	10.0	39.0	8.2	31.1	9.8	4.6	5.5	13.9	8.8	9.8	205.2	19.4	7.1	D
W-14	10	6.0	9.1	10.0	103.7	12.0	5.1	9.2	18.6	2.0	9.4	228.0	23.5	6.8	
W-15	10	5.9	6.1	8.9	132.5	12.2	5.5	12.8	22.9	1.4	9.4	221.6	25.4	6.7	
W-16	10	6.9	15.6	11.7	76.9	9.7	5.0	7.6	18.2	3.5	9.1	221.5	21.4	6.7	
W-17	10	5.9	9.2	8.8	103.3	10.7	4.3	9.7	20.3	2.1	9.4	228.1	23.3	6.6	
W-18	10	7.5	13.5	11.4	101.3	12.8	4.5	10.2	19.7	3.1	9.4	215.1	24.2	6.7	
W-19	10	7.1	5.0	51.5	214.8	33.0	9.0	20.4	43.4	1.1	8.7	222.9	46.8	6.4	
W-20	10	6.9	7.4	31.9	136.9	18.8	6.7	16.6	26.8	1.7	8.8	217.8	34.4	6.6	
Average		12.3	38.9	21.7	57.8	12.6	6.3	8.9	22.1	8.8	9.1	216.0	28.8	7.0	

"N.M." = not measured.

In well type, "S" means shallow well (<30 m deep) and "D" deep well (>30 m deep).

Table 2 Correlation between eight ion contents

	NO_3^-	Cl^-	SO_4^{2-}	HCO_3^-	Na^+	K^+	Mg^{2+}	Ca^{2+}
NO_3^-		0.96	0.66	-0.53	0.26	0.68	0.32	0.59
Cl^-			0.73	-0.44	0.37	0.68	0.41	0.67.
SO_4^{2-}				0.00	0.64	0.66	0.67	0.81
HCO_3^-					0.51	-0.03	0.53	0.22
Na^+						0.52	0.78	0.66
K^+							0.51	0.74
Mg^{2+}								0.80
Ca^{2+}								

Table 3 Results of principal component analysis

	Components	
	Factor 1	Factor 2
Cl^-	0.83	-0.50
NO_3^-	0.77	-0.60
SO_4^{2-}	0.90	-0.02
HCO_3^-	0.05	0.97
Na^+	0.73	0.53
K^+	0.83	-0.11
Mg^{2+}	0.78	0.53
Ca^{2+}	0.92	0.16
Eigenvalues	4.78	2.15
% of variance	59.7	26.8
Cumulative %	59.7	86.5

Table 4 Mean concentrations of respective clusters

	Number of samples	Cl^- (mg L^{-1})	NO_3^- (mg L^{-1})	SO_4^{2-} (mg L^{-1})	HCO_3^- (mg L^{-1})	Na^+ (mg L^{-1})	K^+ (mg L^{-1})	Mg^{2+} (mg L^{-1})	Ca^{2+} (mg L^{-1})
Group 1	60	6.7	9.9	13.6	113.0	13.2	5.3	10.9	21.0
Group 2	11	7.1	5.2	49.7	209.2	31.7	8.8	21.4	44.6
Group 3	81	5.3	11.7	3.8	37.7	7.0	3.7	3.5	9.2
Group 4	125	20.0	73.4	34.7	31.0	14.3	8.3	10.4	28.9

Figure 1

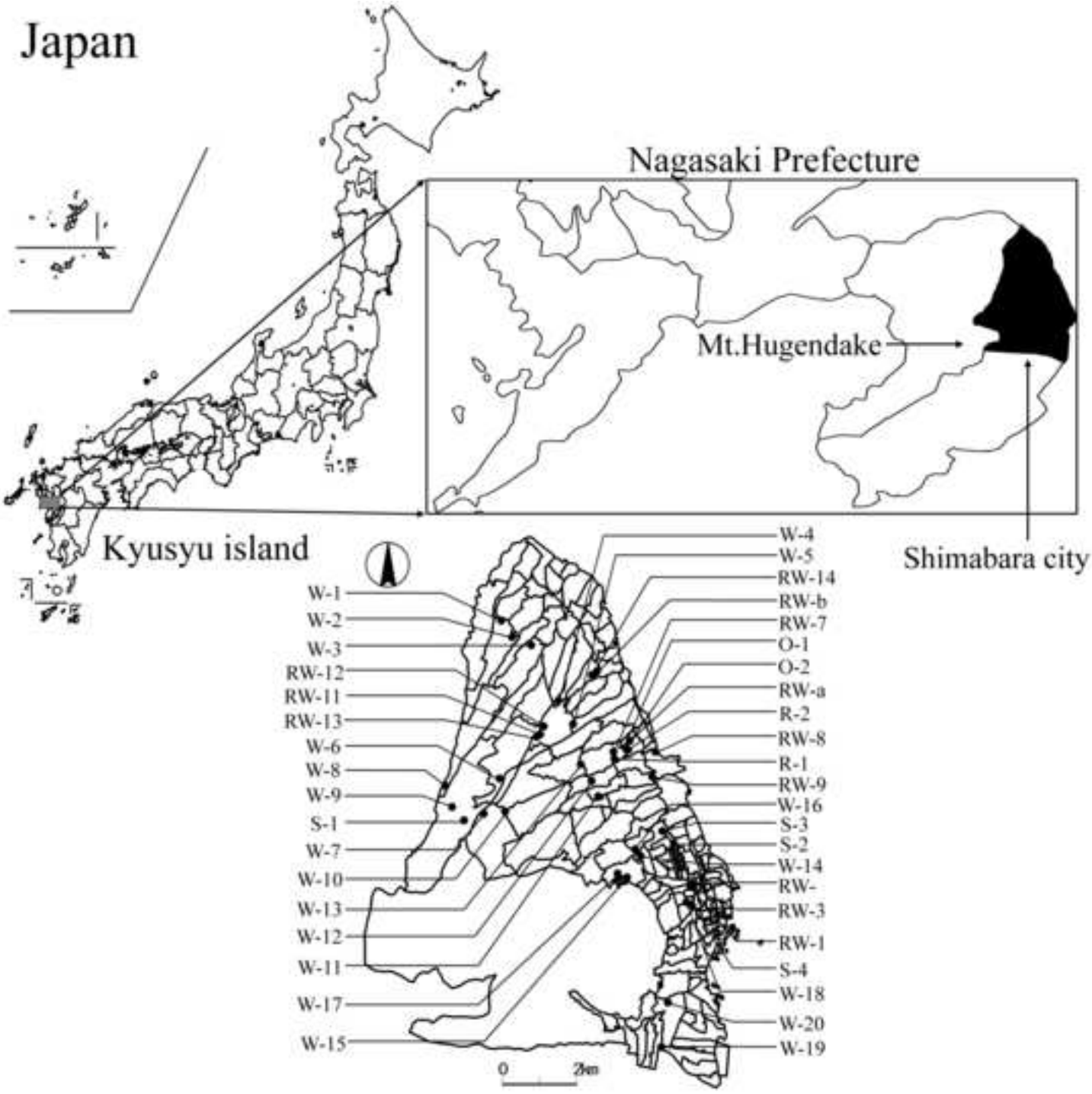
Japan
Nagasaki Prefecture
Mt.Hugendake
Shimabara city
Kyusyu island
W-1
W-2
W-3
RW-12
RW-11
RW-13
W-6
W-8
W-9
S-1
W-7
W-10
W-13
W-12
W-11
W-17
W-15
W-4
W-5
RW-14
RW-b
RW-7
O-1
O-2
RW-a
R-2
RW-8
R-1
RW-9
W-16
S-3
S-2
W-14
RW-
RW-3
RW-1
S-4
W-18
W-20
W-19
0
2km

Figure 2

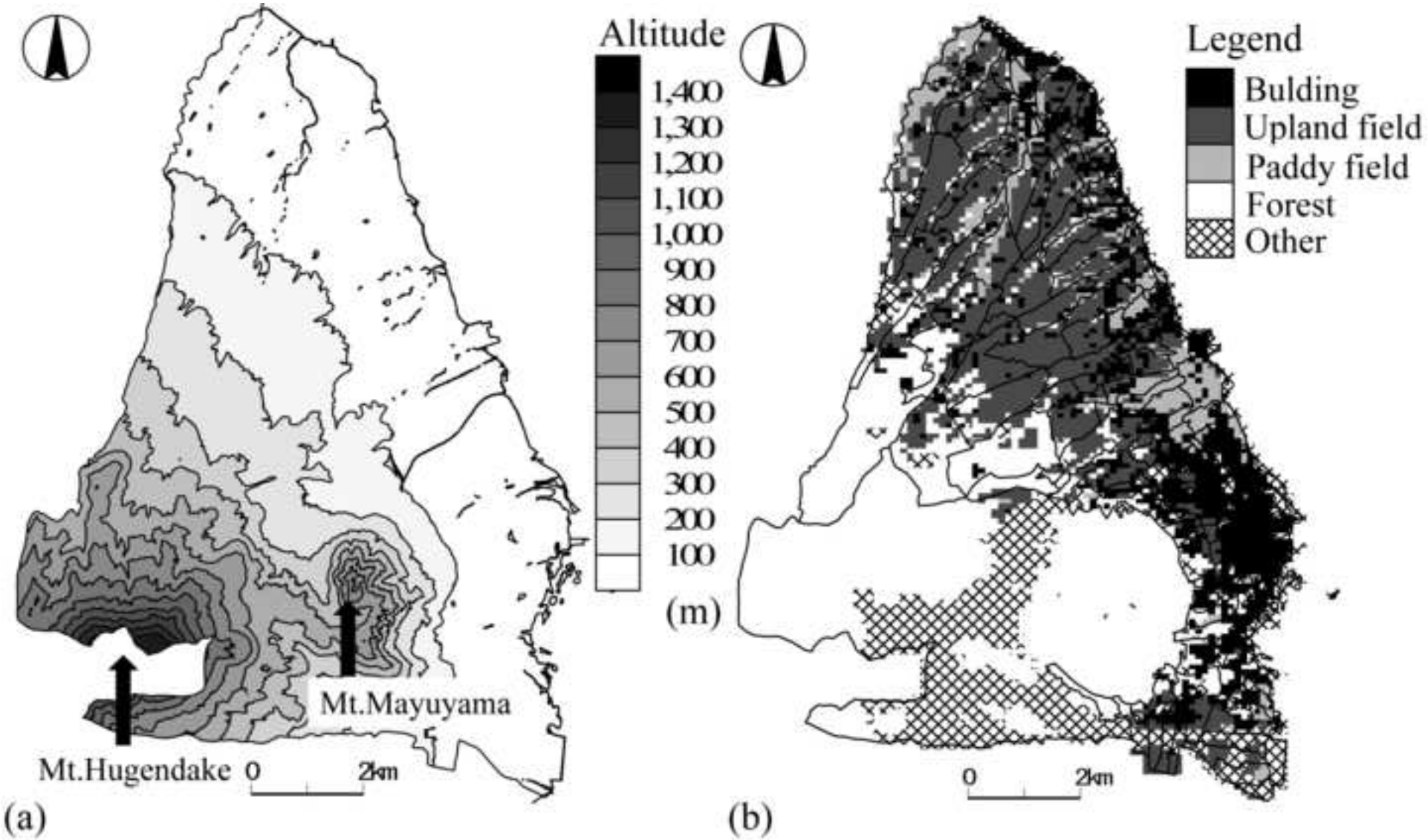
Altitude
1,400
1,300
1,200
1,100
1,000
900
800
700
600
500
400
300
200
100
(m)
Mt.Mayuyama
Mt.Hugendake
0
2km
(a)
Legend
Bulding
Upland field
Paddy field
Forest
Other
0
2km
(b)

Figure 3

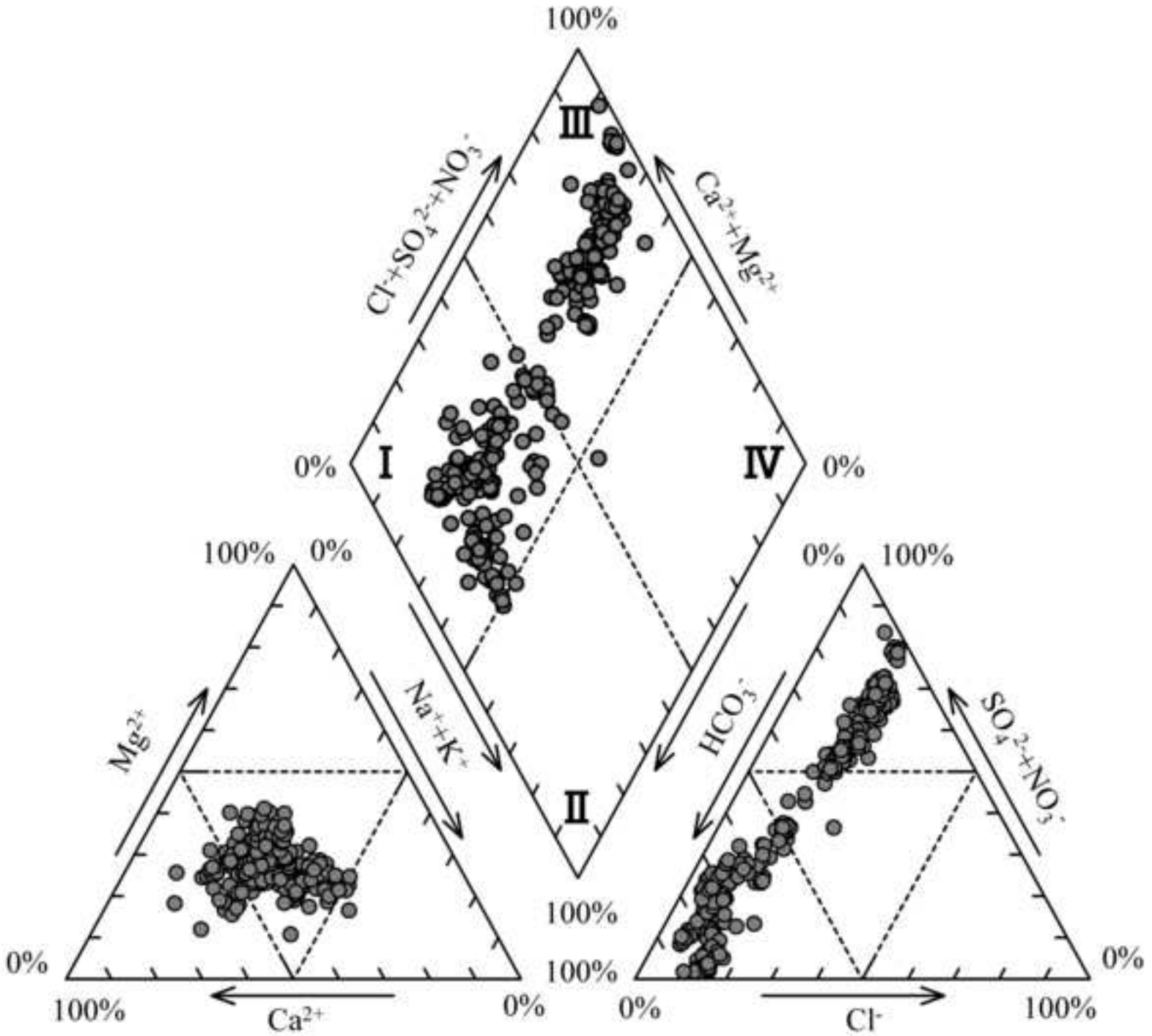
100%
III
$Cl^-+SO_4^{2-}+NO_3^-$
$Ca^{2+}+Mg^{2+}$
0%
I
IV
0%
100%
0%
0%
100%
Mg^{2+}
Na^++K^+
HCO_3^-
$SO_4^{2-}+NO_3^-$
II
100%
100%
0%
0%
100%
0%
100%
Ca^{2+}
Cl^-

Figure 4

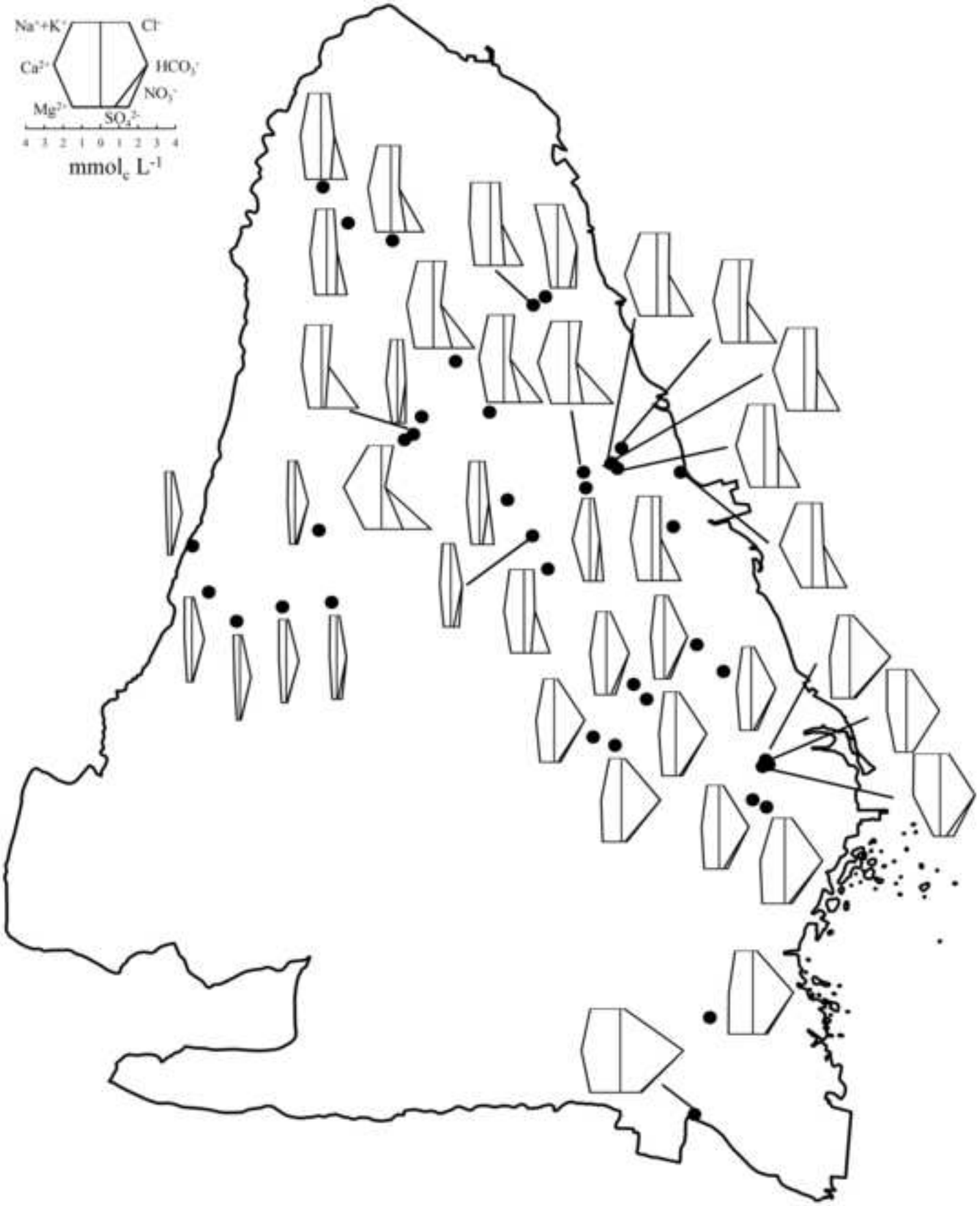

Figure 5

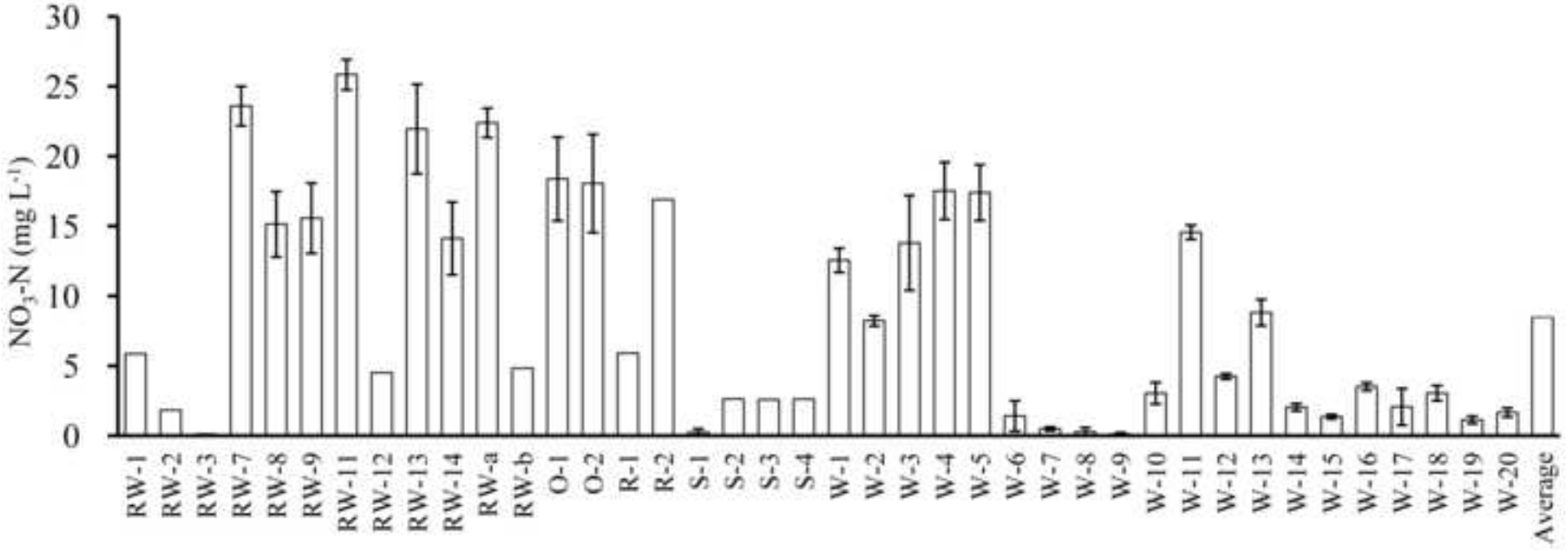
30
25
20
15
10
5
0
NO3-N (mg L-1)
RW-1
RW-2
RW-3
RW-7
RW-8
RW-9
RW-11
RW-12
RW-13
RW-14
RW-a
RW-b
O-1
O-2
R-1
R-2
S-1
S-2
S-3
S-4
W-1
W-2
W-3
W-4
W-5
W-6
W-7
W-8
W-9
W-10
W-11
W-12
W-13
W-14
W-15
W-16
W-17
W-18
W-19
W-20
Average

Figure 6

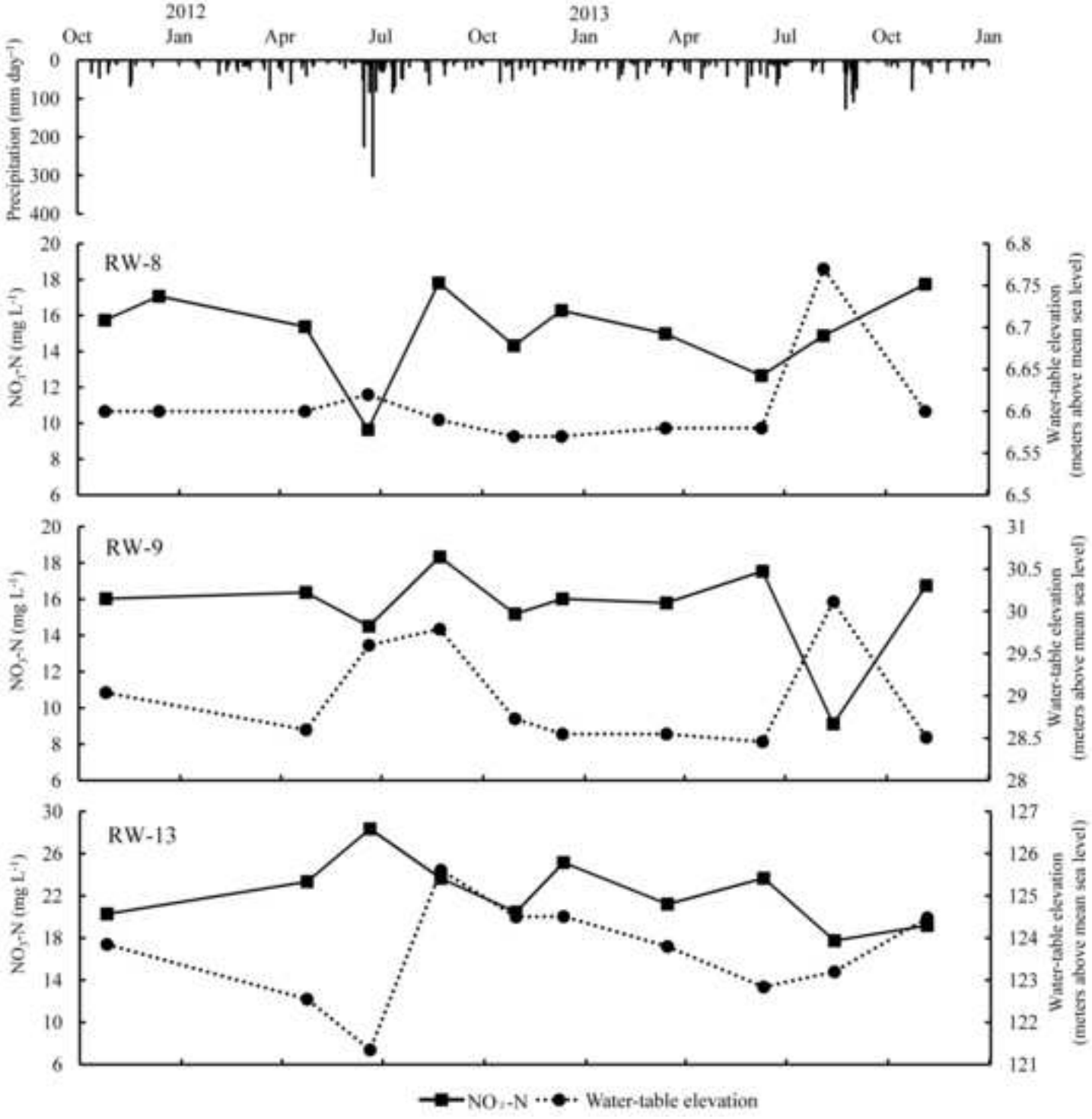
2012
2013
Oct
Jan
Apr
Jul
Oct
Jan
Apr
Jul
Oct
Jan
Precipitation (mm day⁻¹)
0
100
200
300
400
RW-8
RW-9
RW-13
NO3-N (mg L-1)
Water-table elevation (meters above mean sea level)
NO3-N
Water-table elevation

Figure 7

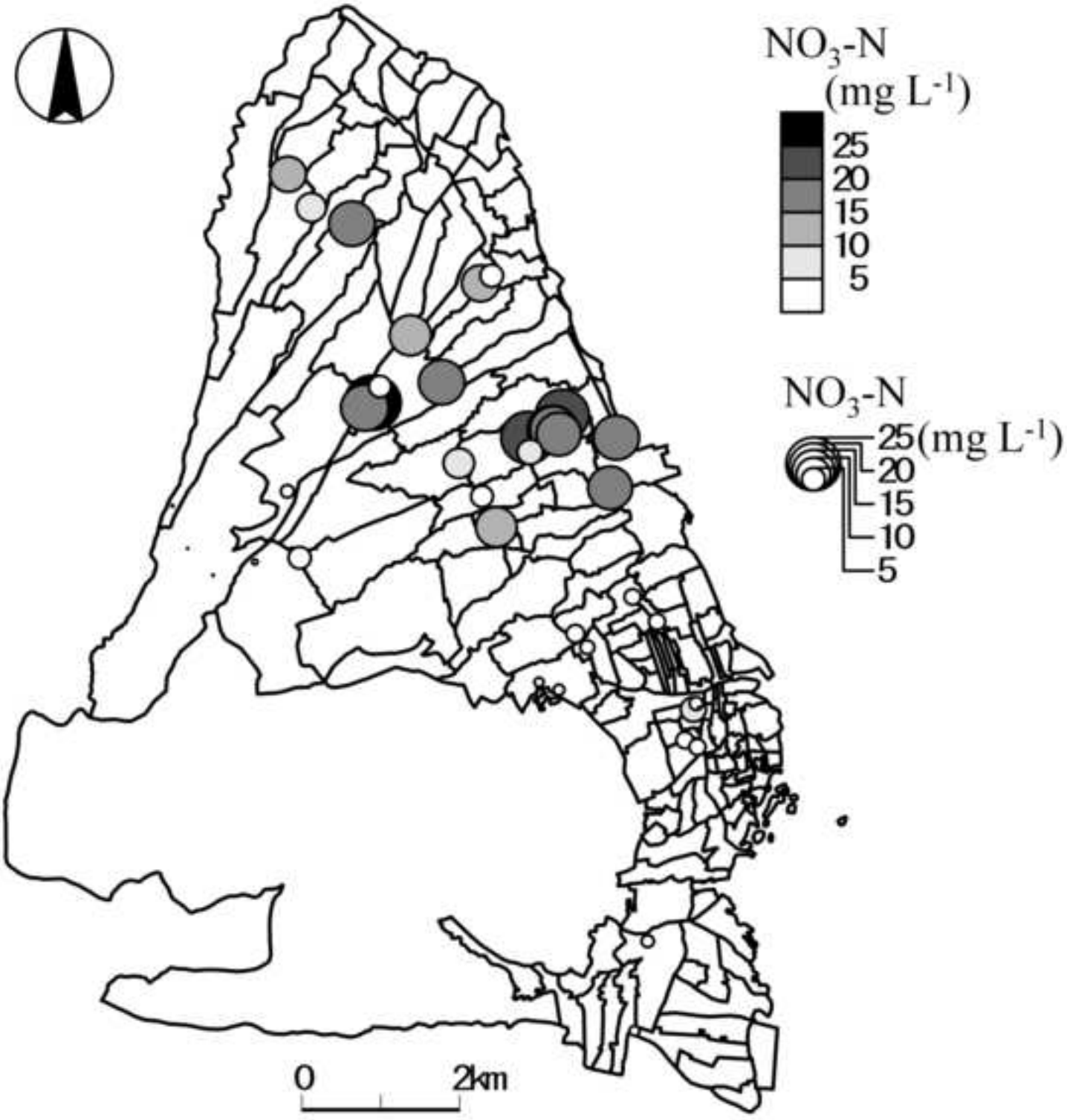

Figure 8

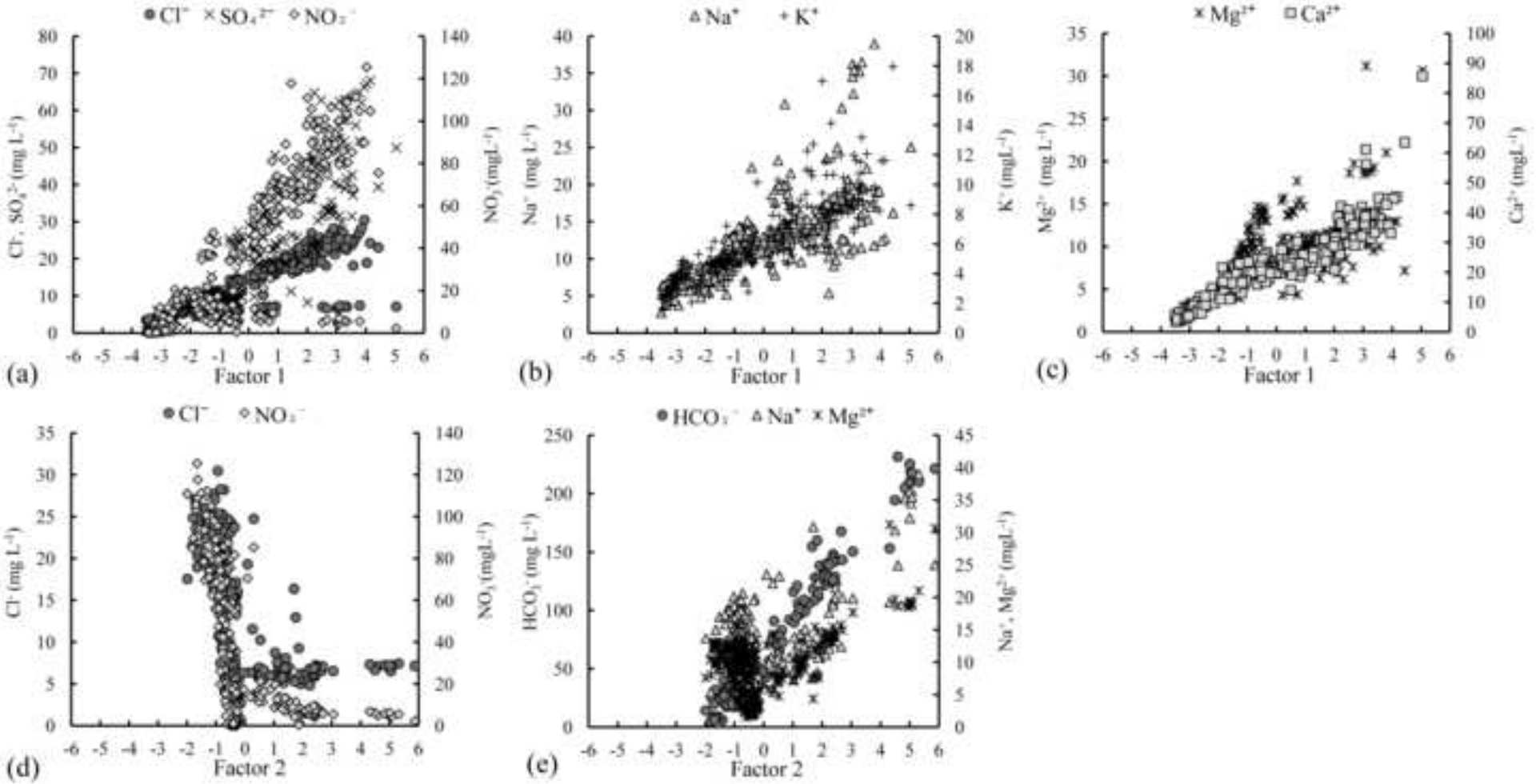
Cl⁻ SO₄²⁻ NO₃⁻
Cl⁻, SO₄²⁻ (mg L⁻¹)
NO₃⁻ (mgL⁻¹)
Factor 1
(a)
Na⁺ K⁺
Na⁺ (mg L⁻¹)
K⁺ (mgL⁻¹)
Factor 1
(b)
Mg²⁺ Ca²⁺
Mg²⁺ (mg L⁻¹)
Ca²⁺ (mgL⁻¹)
Factor 1
(c)
Cl⁻ NO₃⁻
Cl⁻ (mg L⁻¹)
NO₃⁻ (mgL⁻¹)
Factor 2
(d)
HCO₃⁻ Na⁺ Mg²⁺
HCO₃⁻ (mg L⁻¹)
Na⁺, Mg²⁺ (mgL⁻¹)
Factor 2
(e)

Figure 9

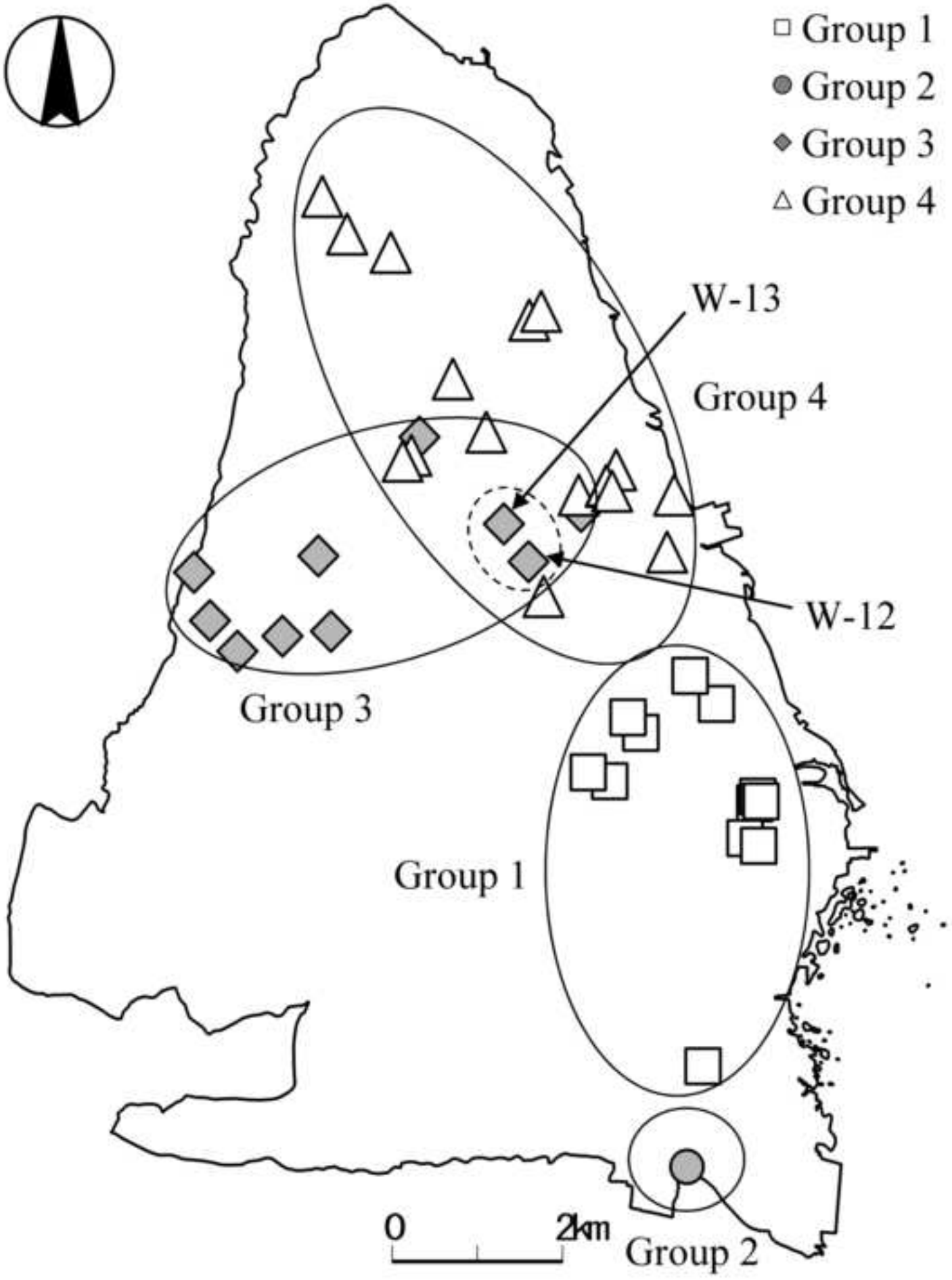
Group 1
Group 2
Group 3
Group 4
W-13
Group 4
W-12
Group 3
Group 1
0
2km
Group 2

Figure 10

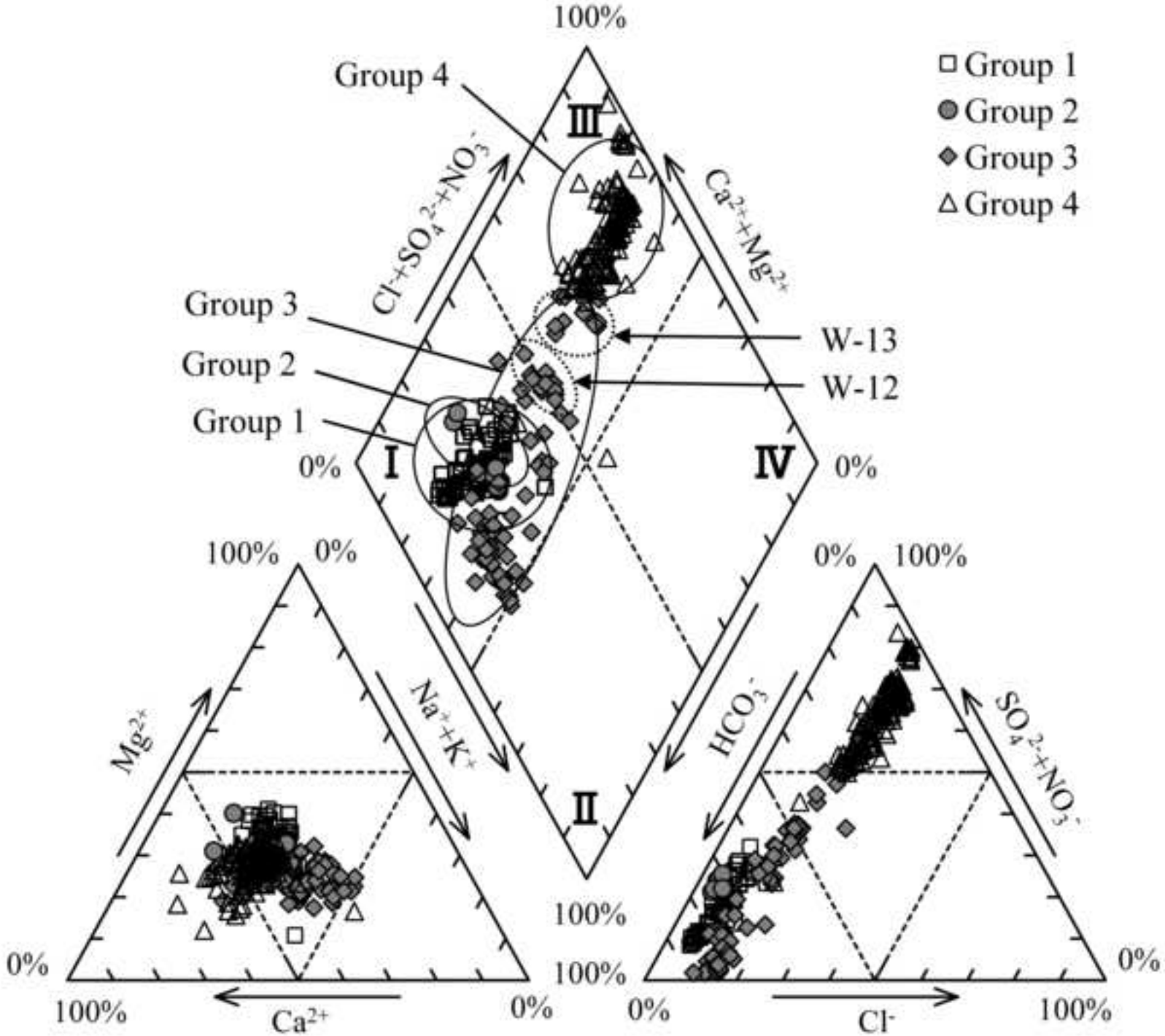
100%
Group 4
III
Group 1
Group 2
Group 3
Group 4
Cl-+SO4 2-+NO3-
Ca2++Mg2+
Group 3
Group 2
Group 1
W-13
W-12
0%
I
IV
0%
100%
0%
0%
100%
Mg2+
Na++K+
HCO3-
SO4 2-+NO3-
II
100%
0%
100%
0%
0%
100%
Ca2+
Cl-

Figure 11

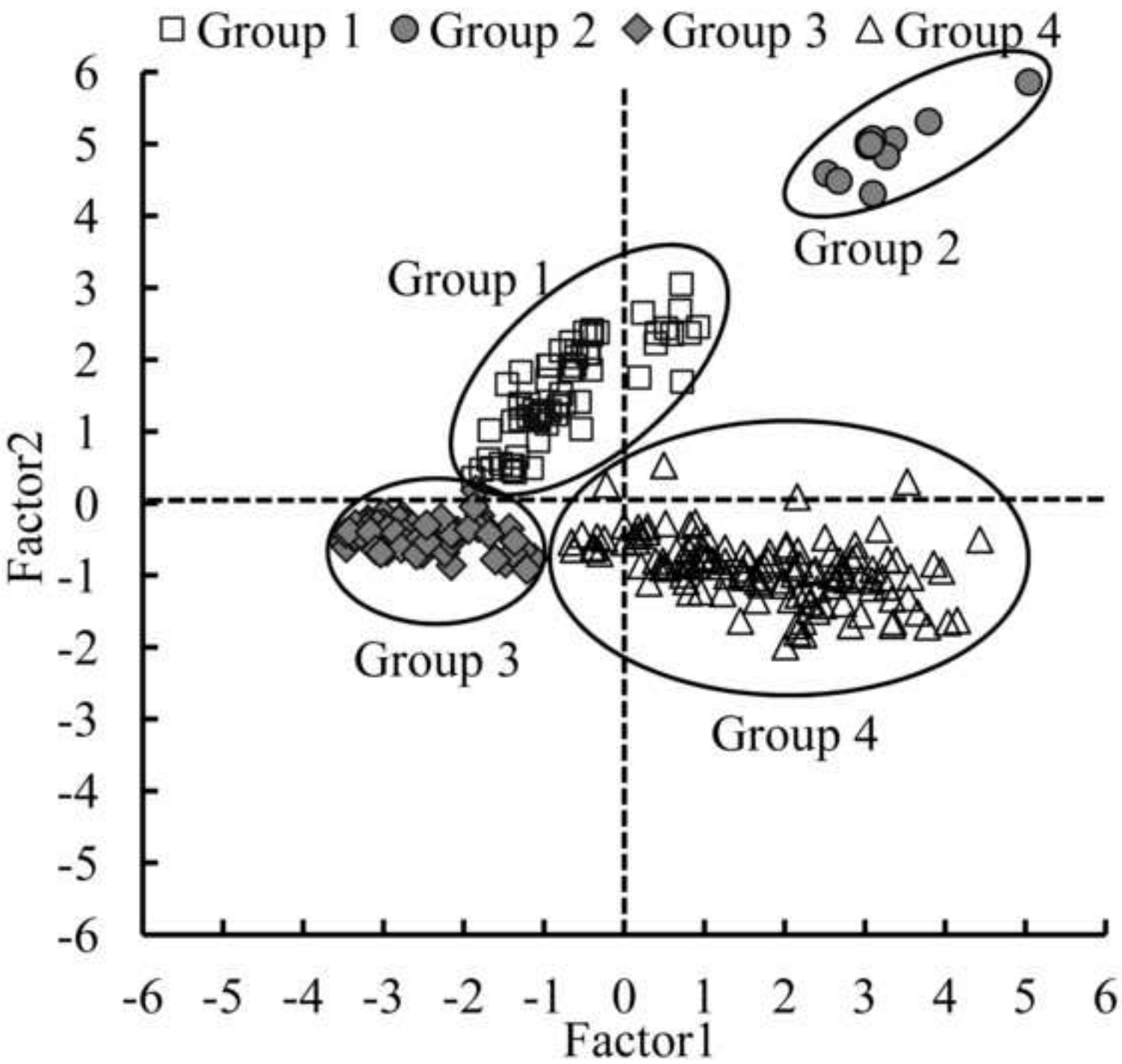
Group 1
Group 2
Group 3
Group 4
Factor2
Factor1
6
5
4
3
2
1
0
-1
-2
-3
-4
-5
-6
-6 -5 -4 -3 -2 -1 0 1 2 3 4 5 6
Group 1
Group 2
Group 3
Group 4